Preprint version

JOURNAL OF PHYSICS AND CHEMISTRY OF SOLIDS

Volume: 123, Pages: 124-132

Impact of disorder on formation of free radicals by gamma-irradiation: multi-frequency EPR studies of trehalose polymorphs

Iva Saric[1*], Jurica Jurec[2], Edward Reijerse[3], Nadica Maltar-Strmečki2, Boris Rakvin[2], Marina Kveder[2]

iva.saric@uniri.hr, Jurica.Jurec@irb.hr, edward.reijerse@cec.mpg.de, Boris.Rakvin@irb.hr, Marina.Ilakovac.Kveder@irb.hr

[1]*Department of Physics and*

[1]*Center for Micro and Nano Sciences and Technologies, University of Rijeka,*

Radmile Matejčić 2, 51000 Rijeka, Croatia

[2] *Ruđer Bošković Institute, Division of Physical Chemistry, Bijenička 54, 10000 Zagreb, Croatia*

[3] *Max Planck Institute for Chemical Energy Conversion, Stiftstrasse 34-36, 45470 Mülheim an der Ruhr, Germany*

Abstract

Electron paramagnetic resonance (EPR) studies of radiation-induced radicals in two anhydrous trehalose polymorphs, beta-crystalline (TRE_c) and glassy (TRE_g), were conducted with the aim to resolve whether different types of free radicals are induced in a differently disordered environment. The multifrequency approach (9.5 GHz, 94 GHz, and 244 GHz) was

applied to improve the *g*-tensor resolution of the complex EPR spectra. In addition, thermal stability of EPR spectra and respective decay kinetics were analyzed in a series of thermal annealing studies in the temperature interval from 333 K to 363 K. It was found that in the crystalline matrix a more complex transformation process of induced radicals is taking place than in the glassy host matrix. Qualitative decomposition of the experimental spectra reproduced essential EPR spectral features in both matrices when 4 contributing radical species were assumed. These were interpreted as carbon-centered radicals while the possibility of formation of alkoxy radicals due to the abstraction of a hydrogen atom was ruled out. Only in one case, tentative assignment of EPR spectral components revealed the formation of the same radical species in both TRE_c and TRE_g. Furthermore, thermal annealing of TRE_g lost one of the radical species, whereas in TRE_c all 4 radical species pertained irrespectively of the treatment. Therefore, the here presented results provide experimental evidence that the extent of disorder present in the material strongly affects the type and stability of radicals induced by ionizing radiation.

Keywords: Trehalose, Irradiation, Multi- frequency EPR, Glassy state

*Corresponding author

1. Introduction

Carbohydrate trehalose, α-D-glucopyranosyl α-D-glucopyranoside, belongs to the molecular glass-forming materials, which are extensively studied both in life sciences as well as in solid-state physics (Scheme 1). In particular, trehalose was shown to be spread in organisms exposed to extreme conditions and assigned as a bioprotective agent responsible for their tolerance of e.g. desiccation/dehydration or cryotemperatures [1]. In this context, the relevant physical property has been attributed in part to trehalose glass transition temperature, which varies as a function of water concentration [2]. In addition, the structure of the trehalose glass and related specific Boson peak properties [3] have been associated with the extensive number of hydrogen bonds realized per one trehalose molecule (16 hydrogen bonds possible per one trehalose molecule) [4, 5]. In such a dense molecular network, clusters of molecules undergo coupled librational dynamics giving rise to Boson peak excitations.

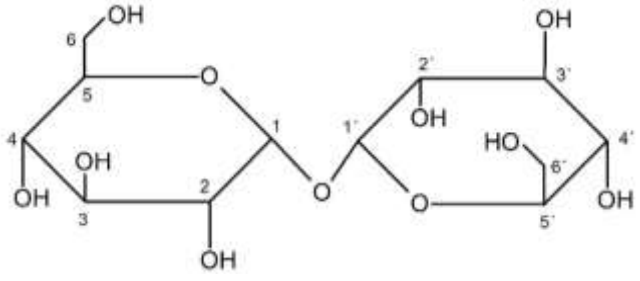

Scheme 1. Trehalose molecule

Many electron paramagnetic resonance (EPR) studies have been conducted on free radicals induced in different types of carbohydrates by ionizing radiation [6-15]. These studies were mainly focused on the determination of the number and structure of induced radicals and on elucidating their mechanisms of formation and decay. Despite all the efforts, the exact assignment of induced radicals was shown to be a very difficult task in carbohydrates in general. Meanwhile, their EPR spectra are often used for dosimetric purposes, as well as for the detection and characterization of sugar containing pharmaceuticals and food products after radiation treatment [16-18]. One additional motivation for investigating complex radiation chemistry of carbohydrates is the clarification of the phenomenon of radiation regioselectivity, i.e. there still exists an open question why radiation causes damage preferentially at certain sites in a molecule [13].

Regarding the so far performed EPR studies on trehalose it should be noted that most of the experiments were performed on trehalose dihydrate single crystals exposed to gamma- or X-radiation [8, 10-14]. The identification of radiation-induced radicals in these studies was done through a combination of EPR techniques like electron nuclear double resonance (ENDOR) and ENDOR-induced EPR (EIE). In addition, a theoretical analysis using an advanced periodic density functional theory (DFT) was performed to calculate the electron magnetic resonance parameters on geometry-optimized radical structures [8, 13]. To investigate the complex transformation mechanisms of the primary radicals to the final stable products, the studies were performed at various temperatures, i.e. 3 K [12], 10 K [14], 77 K [11, 13] and room temperature (RT) [8, 10], using *in situ* irradiation. However, despite these combined experimental/theoretical efforts it is still not possible to unambiguously characterize and identify all the radicals present in an irradiated trehalose dihydrate compound.

The interest in the trehalose molecule in this study comes from a different perspective. In specific, the focus is put on the impact of disorder on the formation of free radicals in the

material exposed to ionizing radiation. To achieve this goal the very same material should be prepared in various polymorphic states. Due to the fact that trehalose is an interesting molecule and can be easily prepared in crystalline and glassy states [19, 20], these polymorphs were chosen as an experimental model system. The motivation for this type of investigation originates from our previous research, which indicated that the processes of thermal decay and formation of radicals are complex and varied from one polymorphic form of trehalose to another [20]. It should be pointed out that during the phase transformation of trehalose initially in the hydrous crystalline form, water molecules evaporate, leaving the final molecule in a chemically different state i.e. the anhydrous form. Therefore, for the current study, both crystalline and glassy trehalose were prepared in the anhydrous state and subsequently exposed to ionizing radiation. This represents an original approach in the EPR study of trehalose radicals.

The aim of this study is to compare two different physical states of anhydrous trehalose, i.e. glassy and crystalline, with respect to the type of free radicals induced by ionizing radiation. Using the beta-trehalose crystalline state as a reference state, the radicals generated in trehalose glass as well as their thermal stability are compared. We rely on EPR spectroscopy in the detection of free radicals whereas the multi-frequency approach is applied to improve the g-tensor resolution and help the tentative assignment of the complex spectra. This interesting physical approach provides the experimental evidence that the extent of disorder present in the material affects the type of radicals induced by ionizing radiation.

2. Materials and methods

2.1. Sample preparation

α,α- Trehalose dihydrate (TRE_d) of 99,99 % purity was purchased from Sigma-Aldrich and used as received. The anhydrous beta crystalline polymorph form of trehalose (TRE_c) was obtained by heating TRE_d in vacuum (500 mbar) at the temperature of 403 K for 4 hours [21]. The glassy state of trehalose (TRE_g) was achieved by heating the TRE_c sample on a hot plate up to the melting temperature of 488 K and subsequent fast quenching of the melt to room temperature. The crystalline and glassy polymorphic states of the prepared samples were verified by differential scanning calorimetry (DSC), as described in our previous work [19].

Both the beta and glassy anhydrous forms of trehalose were gamma-irradiated in air under controlled temperature (293±2) K with a dose of 10 kGy using the panoramic ^{60}Co source of the Ruđer Bošković Institute at the dose rate of 2.8 Gy/s. The irradiation dose in this range is usually applied for investigating sugars and gives EPR signals of appropriate intensity [22].

2.2. Thermal annealing

Three thermal procedures were applied:

a) In order to attain a more stable EPR signal according to the protocol from the literature [10], both TRE_c and TRE_g samples, after exposure to gamma-radiation, were annealed at 313 K for 3 days. These samples are referred as samples b_1 and g_1, respectively.

b) To further explore the thermal stability of samples b_1 and g_1, they were subsequently exposed to the following temperatures: 333 K, 343 K, 353 K, 358 K and 363 K during the EPR measurements in which the signal intensity was followed up to 6 hours.

c) Due to the fact that the EPR spectra exhibit several spectral components [20] the samples b_1 and g_1 were exposed to extreme thermal conditions with the aim to simplify the spectral decomposition. Therefore, after step (a) the b_1 sample was additionally kept at 363 K for 17

hours and the sample is denoted as b_2, whereas the g_1 sample was heated at the same temperature for 2 hours and is denoted as g_2.

It should be stressed that according to the DSC heating thermograms of trehalose polymorphs [19], no phase transitions either in the trehalose beta or glass samples are expected during the thermal annealing procedures applied.

2.3. Multifrequency ESR spectra

The experiments were performed at three microwave frequencies:

a) Continuous-wave (CW) X-band (9.5 GHz) EPR measurements were performed at 293 K using a Varian E-109 spectrometer equipped with a rectangular dual cavity and a Bruker ER 041 XG microwave bridge (9.5 GHz).

Thermal annealing studies were carried out using Bruker TE_{102} rectangular cavity (ER 4102 ST) at the following temperatures 333 K, 343 K, 353 K, 358 K and 363 K. To control the temperature of the sample a variable Chromel-alumel thermocouple was placed in the EPR cavity below the sample. The temperature was controlled within ±1 K using a variable temperature unit Bruker ER 4111 VT with a nitrogen gas flow. The double integrals of the recorded EPR spectra were used to analyze the changes in the signal intensity with time.

b) The W-band (94 GHz) CW EPR spectra were obtained at 100 K by recording the free induction decay (FID) spectra using a Bruker Elexsys E-580 Fourier transform EPR spectrometer. Derivative-type spectra were obtained from the FID spectra by the pseudo-modulation function of the EasySpin software [23].

c) High-field CW spectra were acquired at 293 K on a home-built high-field CW and pulse EPR spectrometer operating at 244 GHz equipped with an ICE-Oxford cryogenic system [24].

The high-field measurements were conducted without a resonator and using induction mode detection.

It should be noted on that the overall shape of the CW EPR spectra does not change essentially within the temperature interval from room temperature to 100 K, thus, for the decomposition of spectral features in terms of tentative radical species the impact of temperature dependent relaxation times was not considered.

The magnetic field calibration for the EPR measurements at 9.5 GHz was performed using the DPPH (2,2- diphenyl-1-picrylhydrazyl, g = 2.0036) standard, whereas at 94 GHz and 244 GHz the procedure was carried out using Mn^{2+} doped MgO as an internal standard as reported [25, 26].

2.4. Qualitative decomposition of ESR spectra

In order to understand the spectral differences between trehalose polymorphs including different sensitivity to thermal annealing procedures, the main issue to address was to resolve whether different types of free radicals are induced in TREc and TREg or the same types of radicals are confined in a differently disordered environment. Therefore, representative trehalose samples b_1 and g_1, exhibiting a stable EPR signal [10, 20] and further annealed at 363 K (Fig. 1, samples b_2 and g_2) were chosen for multi-frequency analysis. The strategy relies on the improved resolution of g-tensor anisotropy with the increase of the applied EPR frequency. Therefore, trehalose EPR spectra were compared at three different frequencies 9.7 GHz, 94 GHz and 244 GHz with the aim to simplify the spectral assignment with respect to the various spectral contributions. EasySpin software package was used for spectral simulation and analysis of EPR spectra based on the esfit routine with function pepper [23]. It should be emphasized that the presented simulations should be primarily

considered as a first qualitative guess of the anhydrous trehalose spectral decomposition based on the EPR signatures of radical types previously published for hydrous trehalose [13, 14] and sucrose [9].

Due to the fact that at 9.7 and 94 GHz the hyperfine couplings and g-tensor resolution showed to be similar and did not allow a straightforward spectral decomposition, data acquired at 244 GHz, although showing less resolved hyperfine couplings due to the g-strain, were appropriate to resolve the largest couplings on the basis of g-tensor differences between radical species. Therefore, simulations of the experimental spectra started in the first run from the data acquired at 244 GHz in order to resolve g-tensor components and then spectral decomposition at lower frequencies was performed. In the second run these g-tensors components were fixed, and the hyperfine couplings estimated at 9.7 GHz were further applied at higher frequencies in order to converge to a self-consistent set of estimated spectral parameters valid at all three frequencies. It should be emphasized that different ratios of spectral contributions observed at different frequencies may be due to the frequency dependent relaxation phenomena and, thus, one should consider them as being informative rather than exact values.

3. Results and discussion

In order to reveal the impact of disorder on the formation of free radicals in the material exposed to ionizing radiation thermal stability and decay kinetics of EPR signals of the two irradiated anhydrous forms of trehalose were analyzed in a series of thermal annealing studies. In addition, the discussion of differences between the radical content in glassy and crystalline trehalose was put into the framework of qualitative decomposition of experimental data.

3.1. Thermal annealing studies

Since the rate of the change of both the intensity and the shape of the EPR spectra of TRE_c and TRE_g irradiated with the same dose is significantly different, characteristic spectra for each sample were chosen to demonstrate different stages of evolution of the respective EPR spectra.

Immediately after the exposure to gamma-irradiation the EPR spectrum of TRE_c exhibits a more complex hyperfine structure as compared to TRE_g (Fig. 1, plots (i)). After annealing the samples for three days at 313 K the EPR spectrum of TRE_c indicates substantial changes (Fig. 1a, sample b_1) as compared to the EPR spectrum of TRE_g (Fig. 1b, sample g_1), which practically remained the same. In the former case the EPR spectrum evolved towards the simplified pattern indicating free radical conversion and decay of species during the annealing procedure. This observation points to the importance of molecular packing of the host matrix exposed to ionizing radiation. With the aim to simplify the spectral assignment of trehalose polymorphs, further thermal annealing of b_1 and g_1 samples, which otherwise exhibit EPR signals stable for at least a year when kept at room temperature [10, 20], was performed at 363 K until the shape of the EPR spectra did not change significantly (Fig 1., plots (iii) and (iv)). During the procedure the spectra became somewhat smoothed but no real simplification with respect to the multicomponent contribution could be observed when comparing the spectra of samples b_1 (g_1) with b_2 (g_2) (Fig. 1). However, when the samples were heated above 363 K both trehalose polymorphs presented EPR spectra drastically changed, ultimately converging to the similar type of a single broad almost structurless EPR line (Fig. 1a and 1b, plots (v)).

To study the EPR spectral changes of trehalose samples b_1 and g_1 in more detail, thermal decay experiments were carried out at various temperatures ranging from 333 K to 363 K, as

shown in Fig. 2. It is interesting to note that the EPR signal intensity of crystalline trehalose remained virtually constant as compared to the glassy trehalose, which exhibited fast thermal decay. At 333 K the EPR signal of the crystalline sample even showed a slight initial increase in intensity pointing to a more complex transformation processes of induced radicals in the crystalline in comparison to the glassy host matrix. As proposed previously [20], this phenomenon reflects the formation of new radicals, recombination, decomposition, or interaction of radicals with neighboring molecules and in the context of this study emphasizes the importance of molecular packing when the material is exposed to the ionizing radiation. In specific, over the period of 6 h the crystalline samples kept at 363 K exhibited a gradual decrease of the EPR signals by 2 %, whereas the EPR signal in the glassy samples decayed by 77% from the initial signal intensity. These results confirm the hypothesis of different interactions, which sustain the stability of radicals in different polymorphic forms of trehalose.

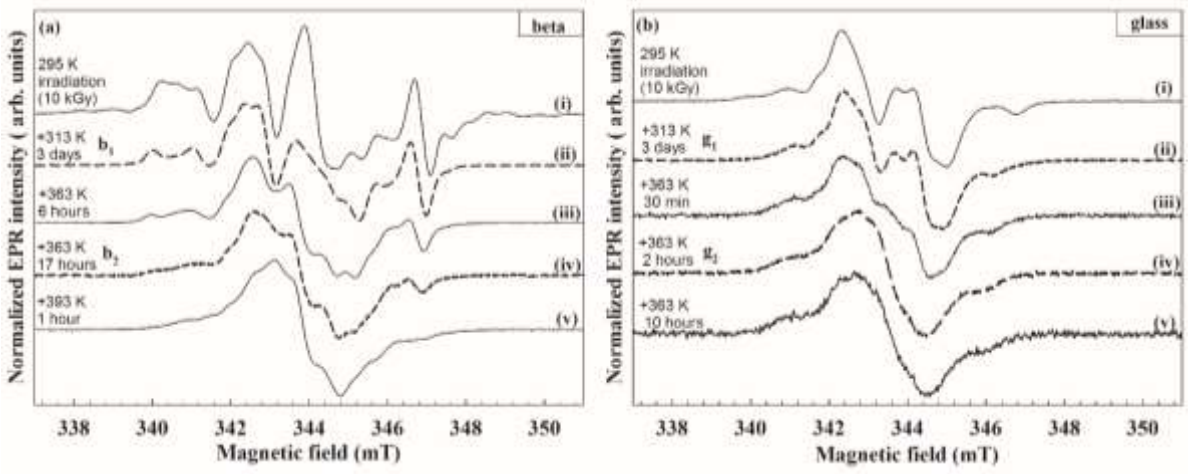

Figure 1. EPR spectra of beta (a) and glassy (b) trehalose exhibiting various thermal annealing histories: (i) immediately after exposure to 10 kGy gamma-irradiation at 295 K; (ii) after subsequent annealing at 313 K for three days (samples denoted as b_1 and g_1, respectively); (iii) after heating of b_1 at 363 K for 6 hours (a) and g_1 for 30 min (b); (iv) after heating of b_1 at 363 K for 17 hours (a) and g_1 for 2 hours (b), (samples denoted as b_2 and g_2, respectively); (v)

after heating of b_2 at 453 K for 1 hour (a), and g_2 at 363 K for 10 hours (b). The dashed spectra labelled b_1, b_2, g_1 and g_2, were chosen for further spectral assignment analysis.

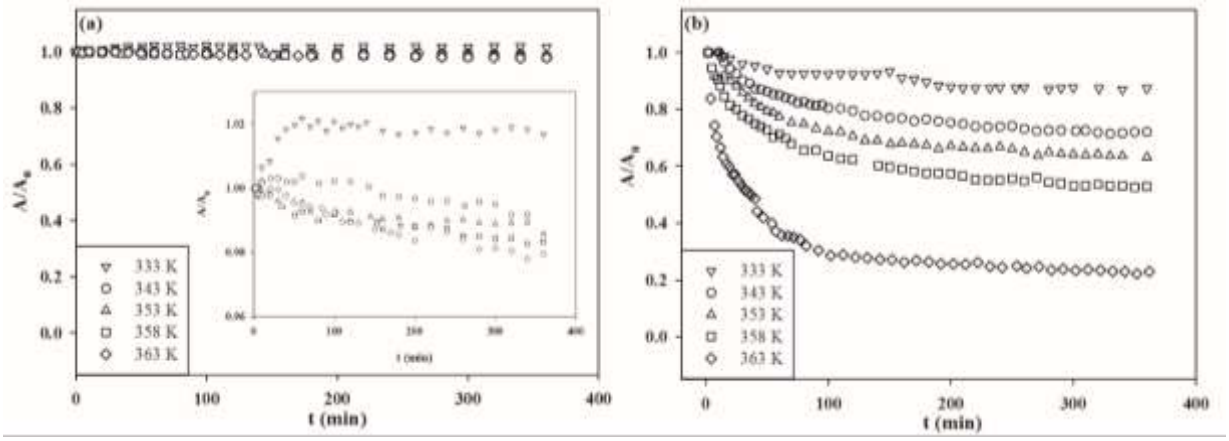

Figure 2. Thermal fading of the EPR signals detected at various temperatures of beta (a) and glassy (b) trehalose exposed to 10 kGy gamma-irradiation at 295 K and subsequently annealed at 313 K for 3 days. A_0 and A represent double integrals of the experimental EPR spectra detected at annealing times $t = 0$ and t, respectively. Inset: Zoom of the scale.

3.2. Multi-frequency ESR spectra analysis: Qualitative assignment of radical's species

A comparison of experimental and simulated EPR spectra of trehalose samples g_1, g_2 and b_1, b_2 at three different frequencies 9.7 GHz, 94 GHz and 244 GHz is shown in Figs. 3 and 4. The qualitative analysis of the EPR spectra resulted in a decomposition of the experimental spectra in spectral components related to paramagnetic centers induced by ionizing radiation in trehalose polymorphs as presented in Tables 1 and 2. In specific, EPR spectra of glassy and crystalline samples were decomposed assuming 4 contributing radical species, $R_1^x, R_2^x, R_3^x, R_4^x$ with x = g_1, g_2, b_1, b_2 (Table 1 and 2, Figs. S1-S12 and Table S1 and S2 in the Supplementary Data), which reproduce the essential features present in the experimental data. It should be emphasized that the presented numerical data should be taken only as a first qualitative attempt towards the understanding of extremely complicated EPR spectra aiming to help the

discussion of differences between the radical content of irradiated anhydrous trehalose polymorphs rather than to be considered as an exact radical assignment values. The approach follows a similar high frequency EPR study of gamma-irradiated sucrose powder, in which three spectral components were reproduced although four of them were realized to be present [9]. It is interesting to note that in the trehalose glass one radical species, $R_4^{g_2}$, is lost by additional heating of the sample whereas in the crystalline sample all 4 radical species pertain irrespectively of the treatment. In addition, the same spectral components R_1, R_2, R_3 contribute to the EPR spectra of both glassy samples (g_1, g_2) whereas for the crystalline samples the EPR parameters for species R_1 vary somewhat between samples b_1 and b_2.

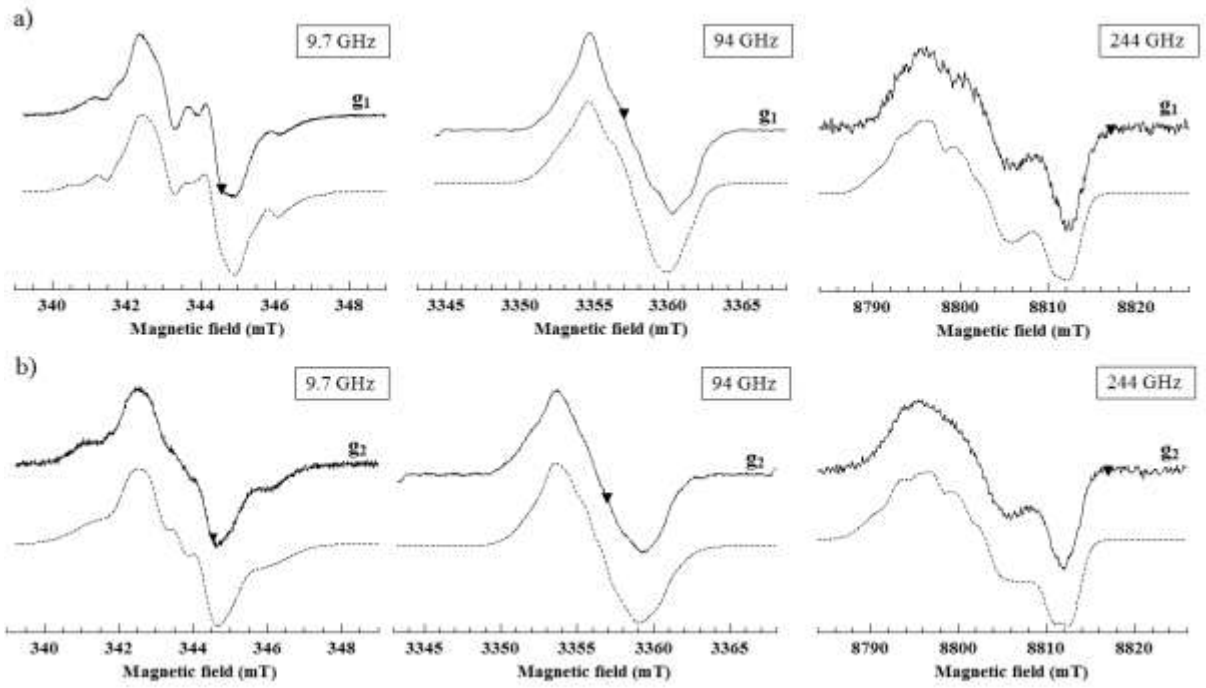

Figure 3. Comparison of experimental (solid line) and simulated (dashed line) EPR spectra of glassy trehalose samples g_1 (a) and g_2 (b) at 9.7 GHz (293 K), 94 GHz (100 K) and 244 GHz (293 K) frequencies. A referent g -value of 2.00101 is indicated by a triangle symbol. The

experimental spectra of samples g_1 (g_2) were simulated assuming 4 (3) spectral components (more details are provided in the Supplementary Data in Figs. S1-S6 and Table 1).

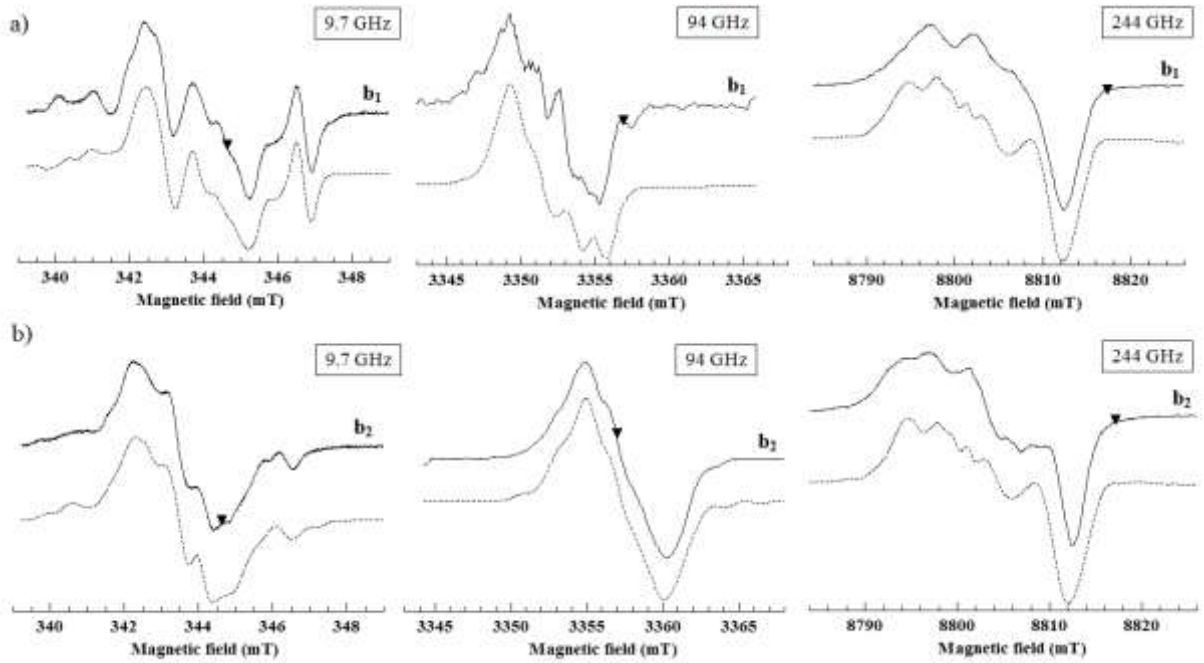

Figure 4. Comparison of experimental (solid line) and simulated (dashed line) EPR spectra of beta trehalose after annealing at 313 K for three days (Fig. 1, b_1 sample) (a) and after heating b_1 for 17 hours (Fig. 1, b_2 sample) (b) at 9.7 GHz (293 K), 94 GHz (100 K) and 244 GHz (293 K) frequencies. A referent $\mathcal{g}$-value of 2.00101 is indicated by a triangle symbol. The experimental spectra of b_1 and b_2 were simulated assuming 4 spectral components (more details are provided in the Supplementary Data in Figs. S7-S12 and Table 2).

It should be emphasized that the assignment of radicals induced in anhydrous trehalose by ionizing radiation to the best of authors' knowledge has never been reported in the literature. Therefore, data available for hydrous trehalose, glucose, and sucrose [6-15] were considered. In addition, a plethora of corresponding radiation products derived from density functional theory (DFT) calculations [6, 13] was inspected and compared with the here presented experimental data (Tables 1 and 2). The rationale behind this comparison is the similarity of

the trehalose molecule, which consists of two glucose units, with the sucrose composed of a glucose and fructose unit. Here presented simulated data for glassy and crystalline trehalose (Table 1 and 2) indicate that the principal values of all the induced paramagnetic center g-tensors, arbitrarily indexed as xx, yy and zz as the principle values of g-tensors, cannot be determined unambiguously on the basis of powder spectra [9] and satisfy the relation $g_{xx} > g_{yy} > g_{zz}$ with only a moderate g-tensor anisotropy ($\Delta(g_{xx} - g_{zz})_{\max} = 0.0067$). This observation implies that the spin density is not dominantly at oxygen atoms but rather that carbon-centered radicals can be anticipated. This observation is in accordance with the data obtained from the multi-frequency study of gamma-irradiated sucrose [9], which rules out the presence of alkoxy radicals or radicals due to the abstraction of a hydroxy hydrogen [8, 13].

Table 1. Principal values of g and proton hyperfine (hf) tensors (isotropic values given in the brackets) regarding interaction with protons for radicals $R_1^{g1,2}$, $R_2^{g1,2}$, $R_3^{g1,2}$ and $R_4^{g1,2}$, derived from simulations of experimental EPR spectra of gamma-irradiated glassy trehalose samples g_1 and g_2 at various EPR frequencies, ν. Tentative assignment of the respective hydrogen (H) and carbon (C) atoms are indicated referring to the Scheme 2. The underlined numbers represent the uncertainty in the last significant digit(s).

Model	axis	g	hf tensor (MHz) H1 atom	hf tensor (MHz) H2 atom	hf tensor (MHz) H3 atom	Weight*	
						ν (GHz)	%
R_1^{g1} H1 (C3) H2 (C1) H3 (O2)	x y z	2.00617 2.00447 2.00221	59.7 72.9 67.2 (66.6)	9.3 11.4 12.1 (10.9)	33.9 -6.1 5.3 (11.0)	9.5 94 244	31 10 50
R_1^{g2} H1 (C3) H2 (C1) H3 (O2)	x y z	2.00617 2.00447 2.00221	59.7 72.9 67.2 (66.6)	9.3 11.4 12.1 (10.9)	33.9 -6.1 5.3 (11.0)	9.5 94 244	42 42 42
R_2^{g1} H1 (C1) H2 (C3) H3 (C5)	x y z	2.00694 2.00388 2.00232	34.5 40.2 -3.1 (23.9)	4.0 -5.2 11.3 (3.4)	16.1 12.7 16.7 (15.2)	9.5 94 244	41 80 39

R_2^{g2} H1 (C1) H2 (C3) H3 (C5)	x y z	2.00694 2.00388 2.00232	34.5 40.2 -3.1 (23.9)	4.0 -5.2 11.3 (3.4)	16.1 12.7 16.7 (15.2)	9.5 94 244	48 48 48
R_3^{g1} H1 (C5) H2 (C6) H3 (O6)	x y z	2.00586 2.00508 2.00211	67.8 51.7 12.7 (44.1)	12.0 9.0 0.1 (7.0)	17.3 -17.4 35.3 (35.2)	9.5 94 244	23 11 10
R_3^{g2} H1 (C5) H2 (C6) H3 (O6)	x y z	2.00586 2.00508 2.00211	67.8 51.7 12.7 (44.1)	12.0 9.0 0.1 (7.0)	17.3 -17.4 35.3 (35.2)	9.5 94 244	11 11 11
R_4^{g1} H1 (C4) H2 (C6) H3 (C6)	x y z	2.00786 2.00537 2.00112	54.0 41.0 48.0 (47.7)	48.0 52.0 42.0 (47.3)	54.0 31.0 67.0 (50.7)	9.5 94 244	5 0.01 0.2

*Estimated weight percentage of the contribution of a component in the total simulated spectrum; one should consider them as being informative rather than exact values.

Table 2. Principal values of g and proton hyperfine (hf) tensors (isotropic values given in the brackets) regarding interaction with protons for radicals $R_1^{b1,2}$, $R_2^{b1,2}$, $R_3^{b1,2}$ and $R_4^{b1,2}$, derived from simulations of experimental EPR spectra of gamma-irradiated beta trehalose samples b_1 and b_2 at various EPR frequencies, ν. Tentative assignment of the respective hydrogen (H) and carbon (C) atoms are indicated referring to the Scheme 3. The underlined numbers represent the uncertainty in the last significant digit(s).

Model	axis	g	hf tensor (MHz) H1 atom	hf tensor (MHz) H2 atom	hf tensor (MHz) H3 atom	Weight*	
						ν (GHz)	%
R_1^{b1} H1 H2 H3	x y z	2.00613 2.00237 2.00229	47.0 36.0 76.0 (53.0)	12.0 39.0 -9.0 (14.0)	3.0 19.0 14.0 (12.0)	9.5 94 244	45 20 37
R_1^{b2} H1 (C3) H2 (O2) H3 (O3)	x y z	2.00613 2.00237 2.00229	45.1 42.9 30.6 (39.5)	12.2 23.2 5.2 (13.5)	7.1 13.8 13.4 (11.4)	9.5 94 244	37 37 37
R_2^{b1}	x y	2.00543 2.00477	43.1 16.5	13.8 -5.0	5.2 24.2	9.5 94	20 26

H1 (C1) H2 (C3) H3 (C5)	z	2.00164	25.5 (28.4)	13.6 (7.5)	23.0 (17.5)	244	9
$\mathbf{R_2}^{\mathbf{b_2}}$ H1 (C1) H2 (C3) H3 (C5)	x y z	2.00543 2.00477 2.00164	43.1 16.5 25.5 (28.4)	13.8 -5.0 16.6 (13.5)	5.2 24.2 23.0 (11.4)	9.5 94 244	9 9 9
$\mathbf{R_3}^{\mathbf{b_1}}$ H1 (C1) H2 (O2) H3 (C4)	x y z	2.00620 2.00400 2.00258	24.2 24.6 24.5 (24.4)	2.5 3.0 3.2 (2.9)	4.5 4.7 4.7 (4.6)	9.5 94 244	18 40 42
$\mathbf{R_3}^{\mathbf{b_2}}$ H1 (C1) H2 (O2) H3 (C4)	x y z	2.00620 2.00400 2.00258	30.9 24.6 19.7 (25.1)	-4.1 4.0 5.4 (1.8)	13.2 0.8 2.9 (5.6)	9.5 94 244	42 42 42
$\mathbf{R_4}^{\mathbf{b_1}}$ H1 (C4') H2 (C6') H3 (C6')	x y z	2.00699 2.00398 1.99918	70.2 80.7 90.9 (80.6)	77.2 82.5 50.9 (70.2)	22.1 -12.1 28.7 (12.9)	9.5 94 244	17 14 12
$\mathbf{R_4}^{\mathbf{b_2}}$ H1 (C4') H2 (C6') H3 (C6')	x y z	2.00699 2.00398 1.99918	81.3 78.2 76.6 (78.7)	67.3 79.1 65.6 (70.7)	5.2 18.6 17.5 (13.8)	9.5 94 244	12 12 12

*Estimated weight percentage of the contribution of a component in the total simulated spectrum; one should consider them as being informative rather than exact values.

The tentative assignment of radical's species based on the data presented in Tables 1 and 2 could be proposed as follows:

a) glassy trehalose

$R_1^{g_{1,2}}$ radical exhibits two hyperfine interactions with very small anisotropy (H1,2) and isotropic values of 67 MHz and 11 MHz, respectively, which can be assigned to the β- or γ-type proton. The third hyperfine interaction (H3) indicates hyperfine anisotropy of ca. 30 MHz that can arise from the proton of the OH group [27]. These data are similar to the experimental and DFT calculations of the radical model in hydrous trehalose assigned to the C2 centered radical due to the H abstraction [14]. In this case the H1 data would correspond to the hyperfine interaction with the proton at C3, H2 data to the proton at C1 and H3 data refer to the proton at O2 atom (structure 1 in Scheme 2).

$R_2^{g_{1,2}}$ radical assignment is not straightforward. Hyperfine interactions are very close to the data reported for the S1 radical in *X*-irradiated sucrose single crystals [28]. The interpretation is done in terms of one α- and two β- protons, which would correspond, to H1 and H2/H3 atoms from the Table 1, respectively, but the specific radical center has not been identified. Rather, a suggestion of a general type of radical was offered (structure 2a in Scheme 2). Due to the fact that an almost isotropic g -tensor close to the DPPH would be expected for this type of structure, it does not represent a satisfying explanation for the here presented data. Experimental and DFT studies of stable radicals in the irradiated sucrose powder offer among other models the possibility of the rupturing of the glycosidic bond and forming of the radical center at the C1 atom [6, 29, 30]. In this case the hyperfine interactions are due to the α-proton at the C1 atom denoted as H1 and two β-protons at C3 and C5 atoms denoted as H2 and H3, respectively (structure 2b in Scheme 2).

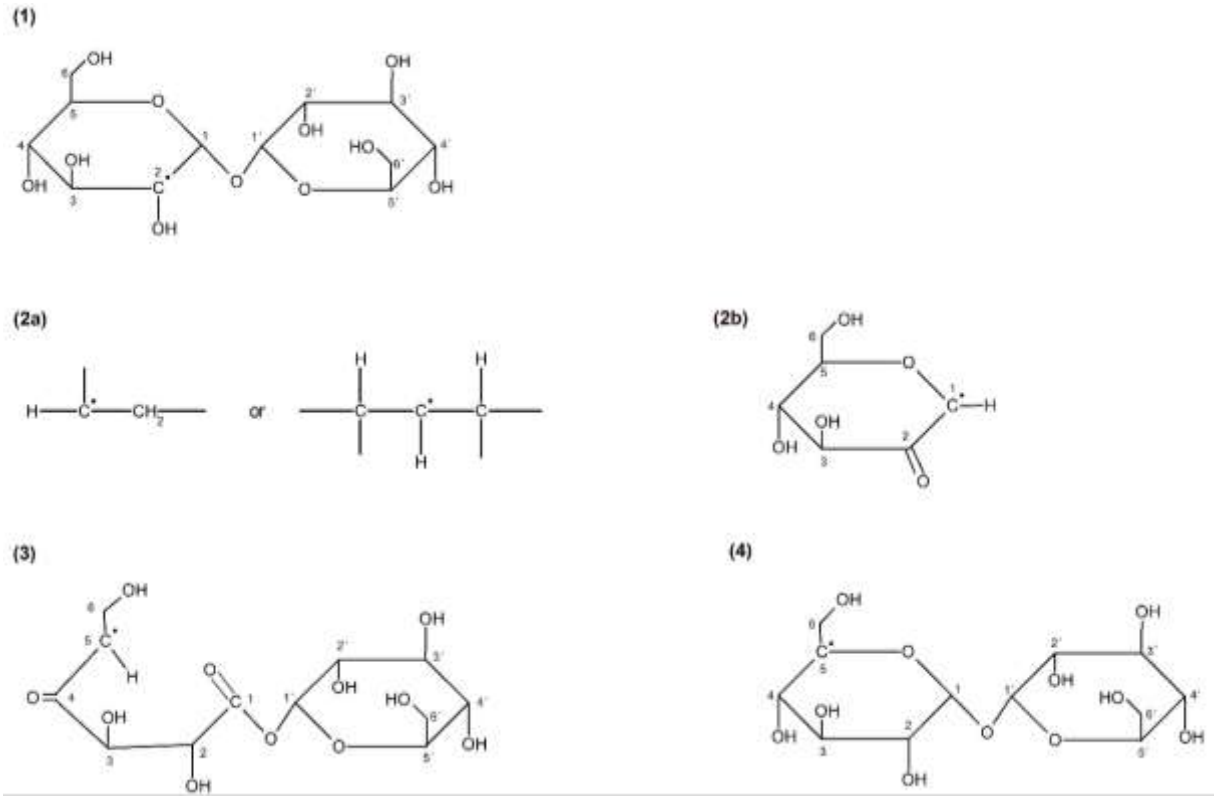

Scheme 2. Tentative assignment of radical species in glassy trehalose.

$R_3^{g_{1,2}}$ radical exhibits one anisotropic hyperfine interaction with an isotropic value of 44 MHz (H1) which might be interpreted as being due to some α- proton. Other hyperfine interactions could be due to some β- or γ- proton (H2) and the proton of the OH group (H3). Referring to the high-frequency EPR study and DFT calculations of stable free radicals in irradiated polycrystalline sucrose [9] the existence of an open ring radical structure of the type originally presented by Sagstuen et al cannot be excluded [31]. This radical model (structure 3 in Scheme 2) explains the somewhat smaller α- proton coupling in terms of unpaired electron delocalization onto the carbonyl oxygen in which case H2 data would refer to the hyperfine interaction with the β- proton at C6 while H3 data with the proton of the O6 atom.

$R_4^{g_{1,2}}$ radical data consists of rather similar three hyperfine interactions: two isotropic hyperfine interactions (H1 and H2) in the range of 48 MHz and the third one somewhat anisotropic (H3) with the isotropic value of 51 MHz. They might be related to the data proposed for the structure of the radical in an irradiated mannose referring to the hydrogen detachment from C5 atom [32]. As presented in structure 4 in Scheme 2 the unpaired electron experiences hyperfine interaction with the proton at C4 and two protons bonded to C6 atom with the values of 53.2 MHz, 53.2 MHz and 42 MHz, respectively [32]. This radical species was also reported in hydrous trehalose irradiated at 10 K [14] but with much larger isotropic couplings of 86 MHz for the proton at C4 atom and 28 MHz for the proton(s) at C6 atom.

b) crystalline trehalose

$R_1^{b_1}$ radical data exhibits one anisotropic hyperfine interaction with the isotropic value of 53 MHz (H1), one hyperfine interaction with the anisotropy of ca. 30 MHz (H2) and the hyperfine interaction of 12 MHz (H3). Tentative assignment of the stable radical of the type presented above for $R_3^{g_1}$ could be proposed (structure 3 in Scheme 2 and structure 1 in

Scheme 3). However, this solution cannot explain its further thermal evolution into the radical of the $R_1^{b_2}$ type, thus, the identity of the $R_1^{b_1}$ will be left open.

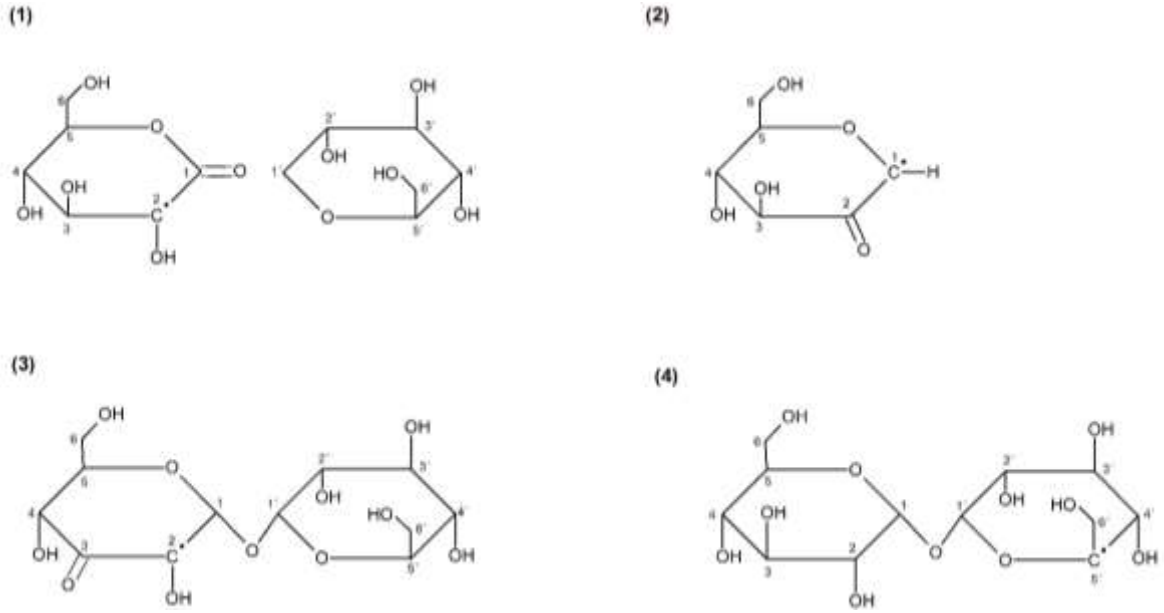

Scheme 3. Tentative assignment of radical species in crystalline trehalose.

$R_1^{b_2}$ radical data exhibit isotropic hyperfine interactions of 40 MHz (H1), 14 MHz (H2) and 11 MHz (H3). Data for H1 proton perfectly fits the experimental data consistent with the model of a stable radical suggested in hydrous trehalose for which β- type proton hyperfine interaction of 39.26 MHz was experimentally derived [8]. It should be pointed out that DFT calculations failed to reproduce these experimental data accurately while the only experimental data available refers to H1 proton [8]. However, the radical center at C2 atom is suggested upon breaking of the glycosidic bond with carbonyl group formation as presented in structure 1 in Scheme 3. Due to the fact that the same type of radical was observed in sucrose powder [6] it is suggested that this mechanism is of general importance in the chemistry of irradiated disaccharides [8]. Therefore, H1 data presented for $R_1^{b_2}$ radical would refer to the hyperfine interaction with the β- proton at C3 while H2 and H3 have to be interpreted as hyperfine interactions with the protons at O2 and O3, respectively.

$R_2^{b_{1,2}}$ radical data show to be rather similar to the hyperfine interactions presented for $R_2^{g_{1,2}}$ in the glassy state (Table 2) implying basically the same radical structure in both glassy and crystalline trehalose induced by irradiation. The interpretation of radical species is in terms of the model assuming rupturing of the glycosidic bond and the formation of the radical at C1 atom (structure 2b in Scheme 2 equal to structure 2 in Scheme 3).

$R_3^{b_{1,2}}$ radical data exhibit isotropic values for all three hyperfine interactions of 24 MHz (H1), 3 MHz (H2) and 5 MHz (H3). Referring to the reported data on room temperature radiation products in trehalose single crystals and DFT analysis [6] a good correspondence with the radical centered at C2 with a carbonyl group at C3 atom can be noticed (structure 3 in Scheme 3). The arguments in favor of this radical assignment are in reported hyperfine interactions, which should be smaller than 15 MHz (two smaller than 10 MHz) along with the enhanced g -tensor anisotropy pointing to ring oxygen in the vicinity of the radical center [6]. In this respect here presented data are consistent with the hyperfine interactions with the protons at C1 (H1), O2 (H2) and C4 (H3) atoms.

$R_4^{b_{1,2}}$ radical data reveal two large fairly isotropic hyperfine interactions (H1, H2), which can be due to two β- type protons, and the third, much smaller hyperfine interaction (H3) as presented in Table 2. Taking into account g -tensor anisotropy (Table 2) and reported data from the literature [14] a very good agreement is found with the model of radical center induced by a net hydrogen abstraction from the C5' atom (structure 4 in Scheme 3). In this case the hyperfine interactions are realized with the protons at C4' (H1) and C6' (H2, H3) atoms.

From the above tentative assignments of EPR spectral components in two different trehalose polymorphs one can notice that only in one case ($R_2^{g_{1,2}}$ and $R_2^{b_{1,2}}$) the formation of the same

radical species was present. The hydrogen abstraction on the atoms C5 (trehalose glass) and C5' (crystalline trehalose) implies somewhat similar damage of the molecule. All the other radical types proposed are shown to be different in the two polymorphs (glassy/crystalline) of trehalose. It should be mentioned that in the field of EPR dosimetry the importance of crystalline, powdered or sintered forms of sugar has been recognized but from the perspective of the sensitivity to the irradiation and the accumulated dose [33]. However, here presented data suggest that different radical species are generated in differently packed molecular structures and, thus, the impact of ionizing radiation is affected by the degree of disorder present in the system exposed to radiation.

4. Conclusion

Here presented results provide experimental evidence that the type and stability of radicals induced by gamma-irradiation in anhydrous trehalose depend on the degree of disorder present in the material. This conclusion was derived from thermal annealing studies in which the rate of the change of both the intensity and the shape of the EPR spectra in TRE_c and TRE_g when irradiated with the same dose was significantly different. In addition, multifrequency EPR spectral analysis resulted in a qualitative decomposition of the experimental spectra in terms of 4 contributing radical species from which only in one case the formation of the same radical species was present in both TRE_c and TRE_g samples, whereas all the other proposed radical types were different. Additional heating of trehalose glass destroyed one radical species, whereas in the crystalline sample all 4 radical species pertained regardless of the treatment. It should be emphasized that here proposed radical types in terms of carbon-centered radicals should be taken only as a first trial in the decomposition of the complex experimental EPR spectra of gamma irradiated anhydrous trehalose. In the

future studies other EPR techniques like ENDOR and ENDOR induced EPR (EIE) should be used to unambiguously identify radicals present in different trehalose polymorphs.

Acknowledgments

The authors highly acknowledge the financial support from the Alexander von Humboldt Foundation. The presented study is a result of the Research Group Linkage Program entitled The study of soft condensed matter by EPR: dynamics in glassy and crystalline matrices. Furthermore, the authors would like to thank Prof. Wolfgang Lubitz (MPI-CEC) for his continuous support for this project. Gudrun Klihm is gratefully acknowledged for her invaluable technical assistance with the high field EPR experiments. The authors thank Dr. Milan Jokić for providing glassy samples. Additionally, the Croatian Science Foundation under the project number 1108 supported this work.

References

[1] S. Magazu, F. Migliardo, M.T.F. Telling, Dynamics of glass-forming bioprotectant systems, J. Non-Cryst. Solids 357 (2011) 691-694.

[2] H.Z. Cummins, H.P. Zhang, J.Y. Oh, J.A. Seo, H.K. Kim, Y.H. Hwang, Y.S. Yang, Y.S. Yu, Y. Inn, The liquid-glass transition in sugars: Relaxation dynamics in trehalose, J. Non-Cryst. Solids 352 (2006) 4464-4474.

[3] O. Yamamuro, K. Takeda, I. Tsukushi, T. Matsuo, Boson peaks in hydrogen-bonded molecular glasses, Physica B-Condensed Matter 311 (2002) 84-89.

[4] G.M. Brown, D.C. Rohrer, B. Berking, C.A. Beevers, R.O. Gould, R. Simpson, Crystal-structure of alpha,alpha-trehalose dihydrate from 3 independent x-ray determinations, Acta Crystallogr. B 28 (1972) 3145-3158.

[5] T. Taga, M. Senma, K. Osaki, Crystal and molecular-structure of trehalose dihydrate, Acta Crystallogr. B 28 (1972) 3258-3263.

[6] H. De Cooman, J. Keysabyl, J. Kusakovskij, A. Van Yperen-De Deyne, M. Waroquier, F. Callens, H. Vrielinck, Dominant stable radicals in irradiated sucrose: g tensors and contribution to the powder electron paramagnetic resonance spectrum, J. Phys. Chem. B 117 (2013) 7169-7178.

[7] H. De Cooman, E. Pauwels, H. Vrielinck, A. Dimitrova, N. Yordanov, E. Sagstuen, M. Waroquier, F. Callens, Radiation-induced defects in sucrose single crystals, revisited: A combined electron magnetic resonance and density functional theory study, Spectrochim. Acta A 69 (2008) 1372-1383.

[8] H. De Cooman, M.A. Tarpan, H. Vrielinck, M. Waroquier, F. Callens, Room temperature radiation products in trehalose single crystals: EMR and DFT analysis, Radiat. Res. 179 (2013) 313-322.

[9] E.R. Georgieva, L. Pardi, G. Jeschke, D. Gatteschi, L. Sorace, N.D. Yordanov, High-field/high-frequency EPR study on stable free radicals formed in sucrose by gamma-irradiation, Free Radic. Res. 40 (2006) 553-563.

[10] A. Graslund, G. Lofroth, Free-radicals in gamma-irradiated single-crystals of trehalose dihydrate and sucrose studied by electron paramagnetic resonance, Acta Chem. Scand. B. 29 (1975) 475-482.

[11] P.O. Samskog, L.D. Kispert, A. Lund, An ESR study of 77 K alkoxy and hydroxyalkyl radicals in x-ray irradiated trehalose single crystals, J. Chem. Phys. 77 (1982) 2330-2335.

[12] P.O. Samskog, L.D. Kispert, A. Lund, Geometric model of trapped electrons in trehalose single crystals x-ray irradiated at 3 K. An EPR study, J. Chem. Phys. 78 (1983) 5790-5794.

[13] M.A. Tarpan, H. De Cooman, E.O. Hole, M. Waroquier, F. Callens, Radiation products at 77 K in trehalose single crystals: EMR and DFT analysis, J. Phys. Chem. A 116 (2012) 3377-3387.

[14] M.A. Tarpan, H. De Cooman, E. Sagstuen, M. Waroquier, F. Callens, Identification of primary free radicals in trehalose dihydrate single crystals X-irradiated at 10 K, Phys. Chem. Chem. Phys. 13 (2011) 11294-11302.

[15] M.A. Tarpan, E. Pauwels, H. Vrielinck, M. Waroquier, F. Callens, Electron magnetic resonance and density functional theory study of room temperature X-irradiated beta-D-fructose single crystals, J. Phys. Chem. A 114 (2010) 12417-12426.

[16] K. Aleksieva, N.D. Yordanov, EPR investigation of some gamma-irradiated excipients, Radiat. Eff. Defect. S. 167 (2012) 685-689.

[17] Z.M. Da Costa, W.M. Pontuschka, L.L. Campos, A comparative study based on dosimetric properties of different sugars, Appl. Radiat. Isot. 62 (2005) 331-336.

[18] P. Fattibene, T.L. Duckworth, M.F. Desrosiers, Critical evaluation of the sugar-EPR dosimetry system, Appl. Radiat. Isot. 47 (1996) 1375-1379.

[19] M. Kveder, I. Saric, D. Merunka, M. Jokic, S. Valic, B. Rakvin, The anhydrous solid trehalose: Low-temperature EPR study of glassy and boson peak modes, J. Non-Cryst. Solids 375 (2013) 19-24.

[20] I. Saric, M. Jokic, B. Rakvin, M. Kveder, N. Maltar-Strmecki, The effect of thermal treatment of radiation-induced EPR signals of different polymorphic forms of trehalose, Appl. Radiat. Isot. 83 (2014) 41-46.

[21] H.J. Reisener, A.S. Perlin, G.A. Ledingham, H.R. Goldschmid, Formation of trehalose and polyols by wheat stem rust (puccinia graminis tritici) uredospores, Can. J. Biochem. Phys. 40 (1962) 1248-1251.

[22] Y. Karakirova, N.D. Yordanov, H. De Cooman, H. Vrielinck, F. Callens, Dosimetric characteristics of different types of saccharides: An EPR and UV spectrometric study, Radiat. Phys. Chem. 79 (2010) 654-659.

[23] S. Stoll, A. Schweiger, EasySpin, a comprehensive software package for spectral simulation and analysis in EPR, J. Magn. Reson. 178 (2006) 42-55.

[24] E. Reijerse, P.P. Schmidt, G. Klihm, W. Lubitz, A CW and pulse EPR spectrometer operating at 122 and 244 GHz using a quasi-optical bridge and a cryogen-free 12 T superconducting magnet, Appl. Magn. Reson. 31 (2007) 611-626.

[25] O. Burghaus, M. Rohrer, T. Gotzinger, M. Plato, K. Mobius, A novel high-field high-frequency EPR and ENDOR spectrometer operating at 3 Mm wavelength, Meas. Sci. Technol. 3 (1992) 765-774.

[26] S. Stoll, A. Gunn, M. Brynda, W. Sughrue, A.C. Kohler, A. Ozarowski, A.J. Fisher, J.C. Lagarias, R.D. Britt, Structure of the biliverdin radical intermediate in phycocyanobilin: Ferredoxin oxidoreductase identified by high-field EPR and DFT, J. Am. Chem. Soc. 131 (2009) 1986-1995.

[27] E. Pauwels, H. De Cooman, G. Vanhaelewyn, E. Sagstuen, F. Callens, M. Waroquier, Radiation-induced radicals in glucose-1-phosphate. II. DFT analysis of structures and possible formation mechanisms, J. Phys. Chem. B 112 (2008) 15054-15063.

[28] G. Vanhaelewyn, J. Sadlo, F. Callens, W. Mondelaers, D. De Frenne, P. Matthys, A decomposition study of the EPR spectrum of irradiated sucrose, Appl. Radiat. Isot. 52 (2000) 1221-1227.

[29] J. Kusakovskij, H. De Cooman, E. Sagstuen, F. Callens, H. Vrielinck, On the identity of the last known stable radical in X-irradiated sucrose, Chem. Phys. Lett. 674 (2017) 6-10.

[30] H. Vrielinck, H. De Cooman, Y. Karakirova, N.D. Yordanov, F. Callens, Early-stage evolution of the EPR spectrum of crystalline sucrose at room temperature after high-dose X irradiation, Radiat. Res. 172 (2009) 226-233.

[31] E. Sagstuen, A. Lund, O. Awadelkarim, M. Lindgren, J. Westerling, Free radicals in x-irradiated single crystals of sucrose: A reexamination, J. Phys. Chem. 90 (1986) 5584-5588.

[32] G.P. Guzik, W. Stachowicz, J. Michalik, EPR study on sugar radicals utilized for detection of radiation treatment of food, Nukleonika 57 (2012) 545-549.

[33] Y. Karakirova, N.D. Yordanov, Sucrose as a dosimetric material for photon and heavy particle radiation: A review, Radiat. Phys. Chem. 110 (2015) 42-50.

Figure captions

Scheme 1. Trehalose molecule

Figure 1. EPR spectra of beta (a) and glassy (b) trehalose exhibiting various thermal annealing histories: (i) immediately after exposure to 10 kGy gamma-irradiation at 295 K; (ii) after

subsequent annealing at 313 K for three days (samples denoted as b_1 and g_1, respectively); (iii) after heating of b_1 at 363 K for 6 hours (a) and g_1 for 30 min (b); (iv) after heating of b_1 at 363 K for 17 hours (a) and g_1 for 2 hours (b), (samples denoted as b_2 and g_2, respectively); (v) after heating of b_2 at 453 K for 1 hour (a), and g_2 at 363 K for 10 hours (b). The dashed spectra labelled b_1, b_2, g_1 and g_2, were chosen for further spectral assignment analysis.

Figure 2. Thermal fading of the EPR signals detected at various temperatures of beta (a) and glassy (b) trehalose exposed to 10 kGy gamma-irradiation at 295 K and subsequently annealed at 313 K for 3 days. A_0 and A represent double integrals of the experimental EPR spectra detected at annealing times $t = 0$ and t, respectively. Inset: Zoom of the scale.

Figure 3. Comparison of experimental (solid line) and simulated (dashed line) EPR spectra of glassy trehalose samples g_1 (a) and g_2 (b) at 9.7 GHz (293 K), 94 GHz (100 K) and 244 GHz (293 K) frequencies. A referent g -value of 2.00101 is indicated by a triangle symbol. The experimental spectra of samples g_1 (g_2) were simulated assuming 4 (3) spectral components (more details are provided in the Supplementary Data in Figs. S1-S6 and Table 1).

Figure 4. Comparison of experimental (solid line) and simulated (dashed line) EPR spectra of beta trehalose after annealing at 313 K for three days (Fig. 1, b_1 sample) (a) and after heating b_1 for 17 hours (Fig. 1, b_2 sample) (b) at 9.7 GHz (293 K), 94 GHz (100 K) and 244 GHz (293 K) frequencies. A referent g -value of 2.00101 is indicated by a triangle symbol. The experimental spectra of b_1 and b_2 were simulated assuming 4 spectral components (more details are provided in the Supplementary Data in Figs. S7-S12 and Table 2).

Scheme 2. Tentative assignment of radical species in glassy trehalose.

Scheme 3. Tentative assignment of radical species in crystalline trehalose.